Particle Growth Modeling of Gas Phase Polymerization of Butadiene

JIANZHONG SUN,[1] CHRISTOPHER EBERSTEIN,[2] KARL-HEINZ REICHERT[2]

[1] Department of Polymer Science and Engineering, Zhejiang University, Hangzhou, 310027, People's Republic of China

[2] Institut für Technische Chemie der Technischen Universität Berlin, Straße des 17. Juni 135, D-10623 Berlin, Germany

Received 28 March 1996; accepted 3 August 1996

ABSTRACT: Butadiene polymerization in the gas phase is modeled by a polymeric multilayer model. Intraparticle mass and heat transfer effects are studied. The effects of catalyst size and diffusivity of butadiene on the radial profile of monomer concentration in polymeric particles and on the rate of particle growth are significant. Intraparticle temperature gradients do appear to be negligible under normal reaction conditions. External boundary layer heat effects are studied for various operation conditions. The model predicts that there is no significant temperature rise of the polymeric particles, even in the case of large catalyst particles. The effect of deactivation of active sites on the rate of particle growth is also studied. © 1997 John Wiley & Sons, Inc. J Appl Polym Sci **64:** 203–212, 1997

Key words: gas phase polymerization; butadiene; modeling; particle growth; concentration and temperature profile

INTRODUCTION

The gas phase polymerization of butadiene by heterogeneous catalysts based on neodymium was studied on a laboratory scale.[1,2] The goal of this study was to establish a mathematical model that would be used to simulate polymeric particle growth and the effect of heat transfer resistance at the external boundary layer of the polymeric particle as well as deactivation phenomena of the catalyst on the growth of polymeric particles for gas phase polymerization of butadiene.

Various models for gas phase polymerization of olefins by heterogeneous catalysis have been established.[3–9] The polymeric flow model and multigrain model are two models that can be used to describe reasonably well the phenomena at the mesoscale level during polymerization using heterogeneous Ziegler–Natta catalysts. The polymeric multilayer model[9] is a versatile model that can be used to simulate heterogeneous and homogeneous Ziegler–Natta polymerization. In this article the idea and principle of a polymeric multilayer model are used. A multilayer model with heat transfer resistance at the polymeric particle boundary layer is developed to simulate the particle growth for the gas phase polymerization of butadiene by heterogeneous catalysis.

POLYMERIC PARTICLE MODEL

The polymeric particle model used for simulation of particle growth of the gas phase polymerization of butadiene by heterogeneous catalysis is schematically shown in Figure 1. This model was originally suggested by Soares and Hamielec.[9] The boundary conditions of their model, however, were somewhat different from that of this model.

In the multilayer model, the particle is divided into concentric spherical layers as in the multigrain model, but microparticles that make up a macroparticle are not considered. At the begin-

Correspondence to: K.-H. Reichert.

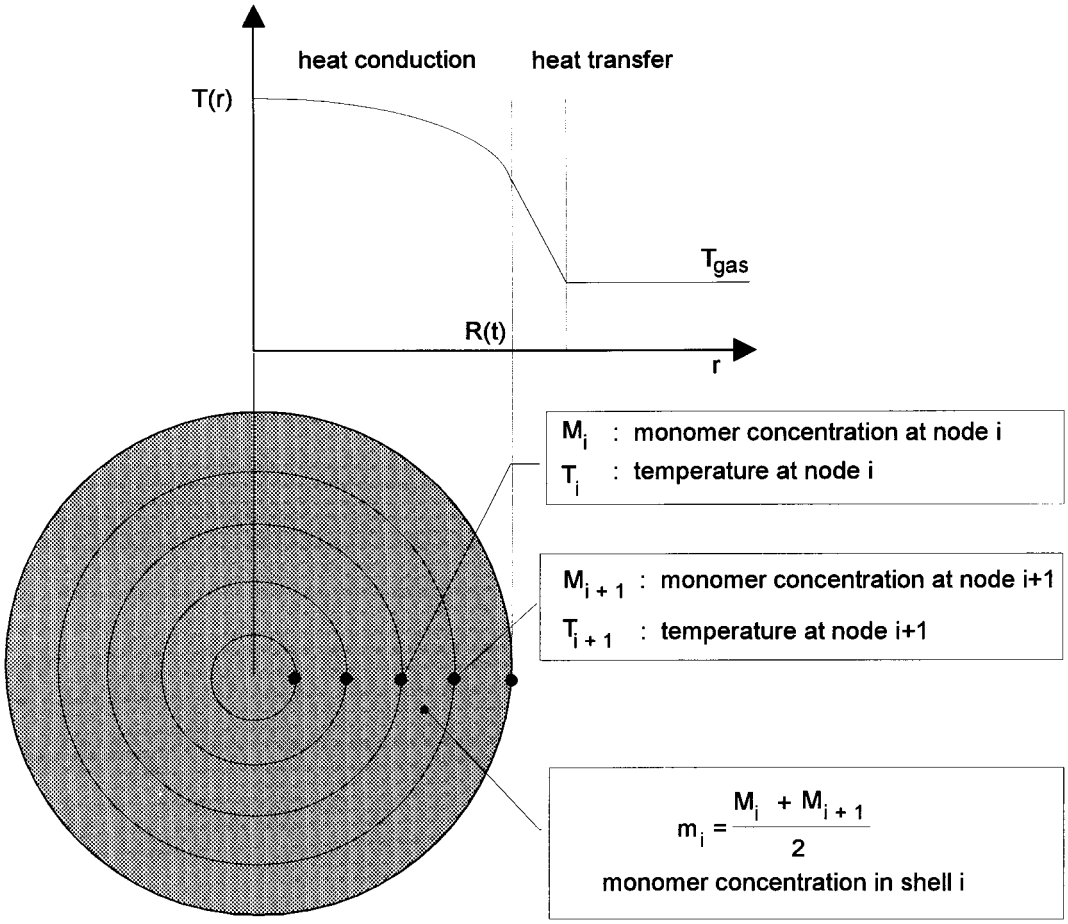

Figure 1 Scheme of the polymeric multilayer model. M_i, monomer concentration at node i; m_i, monomer concentration in shell $i = (M_i + M_{i+1})/2$; T_i, temperature at node i.

ning of the reaction, the concentration of active sites in each layer is the same. The monomer concentration and temperature at the boundaries of each layer (i.e., at each node) are calculated using a 3-point Lagrangian interpolation polynomial method.[10] The rate of polymerization in each layer is calculated by using average concentration and temperature in each time interval. The method of calculation of the average temperature in each layer is similar to that of the average concentration shown in Figure 1. The volume of each layer is updated in terms of the amount of polymer formed in that time interval. The concentration of active sites based on the volume of the layer in each layer is calculated according to the updated volume mentioned above and according to the rate of deactivation of the catalyst, when deactivation of the catalyst is considered. For the next time interval, the process mentioned above is repeated, including recalculation of the monomer and temperature profiles for the new boundary positions.

Material Balance

To model particle growth, the radial profile of monomer concentration in the polymeric particle must be developed. The governing equation of the material balance of the monomer can be described by the diffusion–reaction equation in spherical polar coordinates[11]:

$$\frac{\partial M(r, t)}{\partial t} = \frac{D_e}{r^2}\frac{\partial}{\partial r}\left(r^2 \frac{\partial M}{\partial r}\right) - R_p \qquad (1)$$

where $M(r, t)$ is the monomer concentration in polymeric particle at time t, D_e is the effective diffusion coefficient of the monomer in the polymeric particle, and r is the radial position in the growing polymeric particle. The polymerization rate R_p is given by

$$R_p = k_p C^* \rho_{\text{cat}} M \qquad (2)$$

where k_p is the propagation rate constant given by

$$k_p = k_p^0 \exp(-E_A/R_{\text{gas}}T) \quad (3)$$

Here k_p^0 is the frequency factor of propagation, E_A is the activation energy for propagation, R_{gas} is the gas constant, and T is the temperature of the polymeric particle.

The deactivation of the catalyst can be described by a first-order deactivation[2] according to

$$C^* = C_0^* \exp(-k_d t) \quad (4)$$

with

$$k_d = k_d^0 \exp(-E_D/R_{\text{gas}}T) \quad (5)$$

where t is the reaction time, k_d is the deactivation rate constant of the catalyst, k_d^0 is the frequency factor of deactivation, E_D is the activation energy of deactivation, and C_0^* is the initial concentration of active sites, which is assumed to be equal to the concentration of neodymium fixed at the support and all of the neodymium molecules are assumed to form active sites.

The initial and boundary conditions of eq. (1) are given by

$$M(r, 0) = 0 \quad (6)$$

$$\frac{\partial M(0, t)}{\partial r} = 0 \quad (7)$$

$$M(R, t) = M_0 \quad (8)$$

Energy Balance

$$\rho_p C_p \frac{\partial T(r, t)}{\partial t} = \frac{k_e}{r^2} \frac{\partial}{\partial r}\left(r^2 \frac{\partial T}{\partial r}\right) - Q_p \quad (9)$$

where $T(r, t)$ is the temperature in the polymeric particle, ρ_p and C_p are the density and the heat capacity of the polymeric particle, respectively, and k_e is the thermal conductivity of the polymeric particle. The total heat of polymerization Q_p is expressed as

$$Q_p = (-\Delta H_p) k_p C^* \rho_{\text{cat}} M \quad (10)$$

The boundary and initial conditions are given by

$$T(r, 0) = T_{\text{gas}} \quad (11)$$

$$\frac{\partial T(0, t)}{\partial r} = 0 \quad (12)$$

$$k_e \frac{\partial T(R, t)}{\partial r} = h[T_{\text{gas}} - T(R, t)] \quad (13)$$

where h is the heat transfer coefficient given by the Ranz–Marshall correlation[12] for a single sphere in a fluid moving with relative velocity u. This can be used to reasonably describe the heat transfer process at the external boundary layer[6]:

$$\text{Nu} = 2 + 0.6\ \text{Re}^{1/2}\text{Pr}^{1/2} \quad (14)$$

where $\text{Nu} = h d_p/k_{\text{gas}}$ is the Nusselt number, $\text{Re} = \rho_{\text{gas}} u d_p/\mu_{\text{gas}}$ is the Reynolds number, and $\text{Pr} = \mu_{\text{gas}} C_{p\,\text{gas}}/k_{\text{gas}}$ is the Prandtl number.

The energy balance equation and its boundary and initial conditions, eqs. (9)–(14), must be solved simultaneously with the material balance equation and its boundary and initial conditions, eqs. (1)–(8), to predict the concentration and temperature profiles.

Particle Growth and Grid Updating

The volume and boundary position of each layer must be updated after a predetermined time interval Δt. The monomer concentrations in the previous time step are used in these updatings, and the equations are expressed by

$$V_j^{(0)} = \tfrac{4}{3}\pi[(r_{j+1}^{(0)})^3 - (r_j^{(0)})^3] \quad (15)$$

$$V_j^{(i+1)} = V_j^{(i)}\left[\frac{k_p C_j^{*(i)} M_j M_m \Delta t}{\rho_p} + 1\right] \quad (16)$$

$$r_{j+1}^{(i+1)} = \left[\frac{3}{4\pi} V_j^{(i+1)} + (r_j^{(i+1)})^3\right]^{1/3} \quad (17)$$

where M_m is the molecular weight of the monomer. In these equations, superscripts indicate time and subscripts indicate radial position; for example, $V_j^{(i)}$ and $r_j^{(i)}$ are the volume of layer j and the radial position in growing polymeric particle at the ith time interval, respectively. According to the volume updating, the concentration of active sites based on the volume of layers in layer j at the ith time interval, $C_j^{*(i)}$, is expressed as

$$C_j^{*(i+1)} = C_j^{*(i)} V_j^{(i)}/V_j^{(i+1)} \quad (18)$$

The effect of deactivation on $C_j^{*(i)}$ is described by eqs. (4) and (5).

Numerical Solution

The material and energy balance equations are simultaneously solved by the numerical method. According to a 3-point Lagrangian interpolating polynomial and L'Hôpital's rule (for the situation at the center of the polymeric particle), the radial profile of monomer concentration can be described by

$$\frac{dM(r_k)}{dt} = 2D_e[A_kM(r_{k-1}) + B_kM(r_k) + C_kM(r_{k+1})] - R_p(r_k), \quad k = 2, N-2 \quad (19)$$

$$\frac{dM(r_0)}{dt} = D_e[B_0M(r_0) - B_0M(r_1)] - R_p(r_0) \quad (20)$$

where the radial discretization weights are expressed by

$$A_j = \frac{2r_j - r_{j+1}}{r_j(r_{j-1} - r_j)(r_{j-1} - r_{j+1})} \qquad j = 2, N-2 \quad (21)$$

$$B_j = \frac{3r_j - r_{j+1} - r_{j-1}}{r_j(r_j - r_{j-1})(r_j - r_{j+1})} \qquad j = 2, N-2 \quad (22)$$

$$C_j = \frac{2r_j - r_{j-1}}{r_j(r_{j+1} - r_{j-1})(r_{j+1} - r_j)} \qquad j = 2, N-2 \quad (23)$$

$$B_0 = -\frac{6}{(r_1 - r_0)^2} \quad (24)$$

where N is the total number of grid points or the number of layers plus 1.

The same approach is used for the radial profile of temperature at the interior points and the center of the polymeric particle. The resulting equations are expressed as

$$\frac{dT(r_k)}{dt} = 2\frac{k_e}{C_p\rho_p}[A_kT(r_{k-1}) + B_kT(r_k) + C_kT(r_{k+1})] - \frac{Q_p(r_k)}{C_p\rho_p}, \quad k = 2, N-3 \quad (25)$$

$$\frac{dT(r_0)}{dt} = \frac{k_e}{C_p\rho_p}[B_0T(r_0)] - B_0T(r_1)] - \frac{Q_p(r_0)}{C_p\rho_p} \quad (26)$$

Expanding T in a Taylor series around the outermost point, and using the boundary condition, eq. (13), the second derivative can be obtained and the temperature profile at the outermost point is expressed as

$$\frac{dT(r_{N-1})}{dt} = \frac{2k_e}{C_p\rho_p}\left\{\frac{r_{N-2}}{r_{N-1}(r_{N-1} - r_{N-2})^2}T(r_{N-2}) - \left[\frac{r_{N-2}}{r_{N-1}(r_{N-1} - r_{N-2})^2} + \frac{h}{k_e(r_{N-1} - r_{N-2})}\right]T(r_{N-1})\right\} + \frac{Q_p}{C_p\rho_p} \quad (27)$$

The model can now be directly solved provided that the differential forms of dM/dt and dT/dt to time are made.

Particle Parameter Values

In the analysis to follow, the practical conclusions will depend on the range of parameter values one might encounter for a polymeric particle. For the gas phase polymerization of butadiene, these values are tabulated in Table I. The density and the heat capacity of polymeric particles ρ_p and C_p can be obtained in terms of the density of the polymer ρ_{BR} and the density of the catalyst ρ_{cat}, the heat capacity of the polymer C_{PBR} and the heat capacity of the catalyst C_{pcat}, and the ratio of the volume of the catalyst to that of the polymer in each layer at each time interval, respectively. In fact, the simulation shows that ρ_p and C_p are almost the values of the polymer after a comparative short reaction time. The thermal conductivity of the polymer k_{BR} is used as the thermal conductivity of the polymeric particle.

SIMULATION AND DISCUSSION

Monomer Concentration Profile

The model was used first to evaluate the importance of intraparticle mass transfer resistance. The radial profiles of butadiene concentration are shown in Figure 2 with different effective diffusion coefficients D_e for a catalyst particle with radius of 25 μm; Φ is the initial Thiele modulus $(R_0\sqrt{k_pC_0^*\rho_{cat}/D_e})$. The lowest value of diffusivity

Table I Reaction Conditions and Thermal, Physical, and Transport Properties for Gas Phase Polymerization of Butadiene

Property	Value	Reference
M_0 (mol/m^3)	74.42 ~ 104.59	1
T_0 (K)	293 ~ 323	1
P_{BD} (Pa)	$2 \times 10^5 \sim 2.7 \times 10^5$	1
ΔH_p (J/mol)	73000	13
C_{PBR} (J/kg K)	1600	13
C_{pcat} (J/kg K)	1000	13
k_{BR} (W/m K)	0.15	14
ρ_{BR} (kg/m^3)	890	13
D_e (m^2/s)[a]	$10^{-11} \sim 10^{-9}$	
R_0 (μm)	10 ~ 50	2
k_P^0 (m^3/mol sites s)	1.6×10^9	2
k_d^0 (1/s)	1.5×10^4	2
C_0^* (mol sites/kg cat)	1.8×10^{-1}	2
E_D (J/mol)	5×10^4	2
E_A (J/mol)	2.4×10^4	2
C_{pgas} (J/kg K)	1681	16
μ_{gas} (Pa s)	$7.8 \times 10^{-6} \sim 8.5 \times 10^{-6}$	16
ρ_{gas} (kg/m^3)	4.108 ~ 5.4246	16
ρ_{cat} (kg/m^3)[b]	623	
k_{gas} (W/m K)	0.015 ~ 0.021	16

[a] The lowest value correspondences to the molecular diffusion coefficient of butadiene in polybutadiene.[15]

[b] Calculated using the data provided by the producer of the catalyst.

D_m ($=2 \times 10^{-11}$ m^2/s) is the experimental value[15] of molecular diffusivity. The values of the effective diffusion coefficient are about 10–50 times that of the molecular diffusivity.

In general, the radius of the catalyst has a significant effect on mass transfer resistance and polymeric particle growth. The radial profile of monomer concentration with different radii of the catalyst particles are shown in Figure 3. It can be seen that at the same reaction time and same D_e, the radial profiles of monomer concentration in the polymeric particle with a large catalyst particle are steeper than that with a small catalyst particle; that is, the mass transfer limitation of a polymeric particle with a large catalyst particle is more serious than that of a polymeric particle with a small catalyst particle.

Figure 4 shows the effect of reaction time on the radial profile of monomer concentration. The symbols on the curves indicate the layer limits used for the simulation. The steep radial profile of the butadiene causes the layers to expand at very different rates during the simulation. At time zero all layers have the same spacing. After 30 min of simulation, only the outer layers expand significantly, especially for low D_e and the large catalyst particle because the monomer is not reaching the center of the particle. After a longer time, however, the radial profile of the monomer concentration flattens and the inner layers start to expand at a higher rate. From this simulation result it is reasonable to say that during a comparative long reaction time the inner layers find themselves in a starvation position for monomer under the conditions of a large catalyst particle. Figures 3 and 4 show that there are serious mass transfer limitations due to the large catalyst particle and low effective diffusion coefficient (i.e., high Thiele modulus), which will likely lead to a broad molecular weight distribution.

Temperature Profile

Because the heat transfer resistance at the boundary layer of the polymeric particle is considered in this model, it is convenient to simulate the influence of particle parameter values and external heat transfer resistance on the radial profile of temperature in the polymeric particle and on the temperature rise of the polymeric particle as compared to the temperature of the bulk of the gas phase. The temperature rise of the polymeric particle versus reaction time is shown in Figure 5. (T_c and T_{gas} are the temperature at the center of the particle and the bulk of the gas phase, respectively.) For the gas phase polymerization of butadiene at the conditions given, no serious temperature rise is expected, even in the case of a large catalyst particle.

Figure 6 is the radial profile of the temperature of the polymeric particle at different reaction times. Figure 6 shows that for the gas phase polymerization of butadiene the radial profile of temperature in the polymeric particle is almost uniform with the particle parameter values and the conditions discussed in this article.

Polymeric Particle Growth

Figure 7 presents the rate profile of particle growth for three different levels of initial Thiele modulus. The figure shows that at the same propagation rate constant and concentration of active sites, the particle growth with low initial Thiele modulus (i.e., small catalyst particle and high diffusion coefficient) is faster than that with high

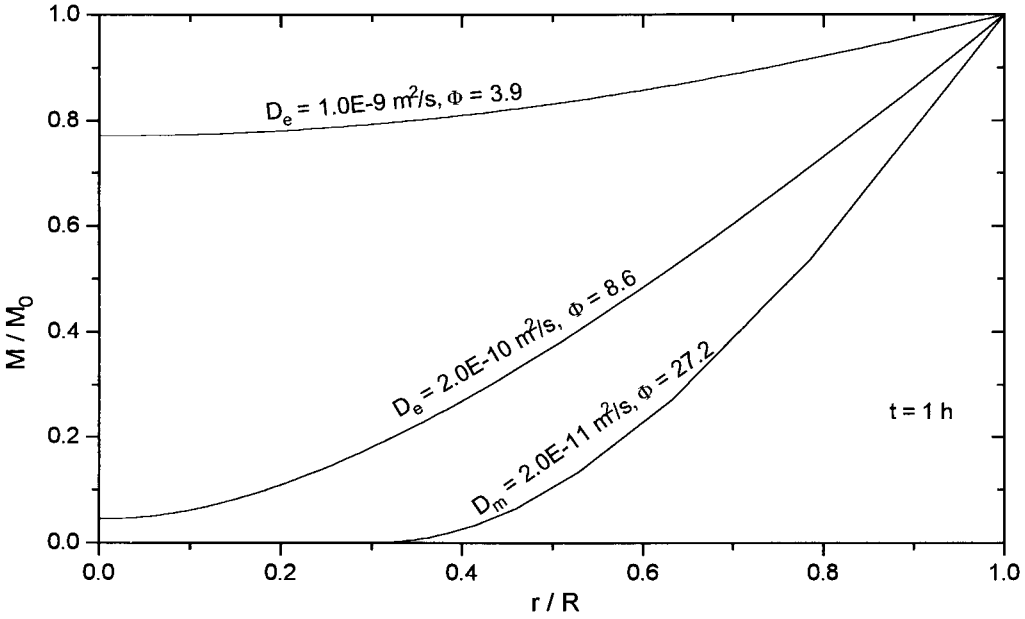

Figure 2 Effect of effective diffusion coefficient on the radial profiles of butadiene in polymeric particle. $k_p^0 = 1.6 \times 10^9$ m^3/s mol sites, $E_A = 2.4 \times 10^4$ J/mol, $C_0^* = 1.8 \times 10^{-1}$ mol sites/kg cat, $R_0 = 25$ μm, $T_{gas} = 323$ K, $p_{BD} = 2.35 \times 10^5$ Pa.

initial Thiele modulus (i.e., large catalyst particle and low diffusion coefficient).

Figure 8 is the comparison of the simulation results with the experimental result of polymeric particle growth. The experimental curve in Figure 8 was obtained using a microreactor for gas phase polymerization of butadiene.[1] The initial mass of catalyst particles with average radius of 25 μm in the reactor was about 0.001 g. The initial temperature of the gas phase was 297 K. The partial pressure of butadiene was 2.7 bar. When polymerization began, the rate of growth of one particle

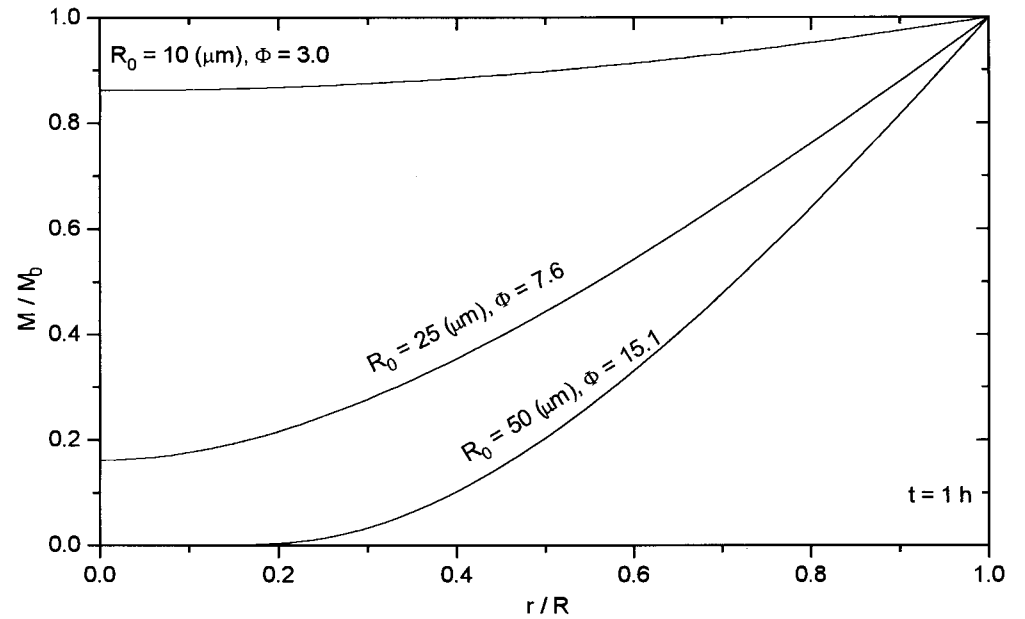

Figure 3 Effect of radius of catalyst on the radial profiles of butadiene in polymeric particle. $k_p^0 = 1.6 \times 10^9$ m^3/s mol sites, $E_A = 2.4 \times 10^4$ J/mol, $C_0^* = 1.8 \times 10^{-1}$ mol sites/kg cat, $T_{gas} = 323$ K, $p_{BD} = 2.35 \times 10^5$ Pa, $D_e = 2.6 \times 10^{-10}$ m^2/s.

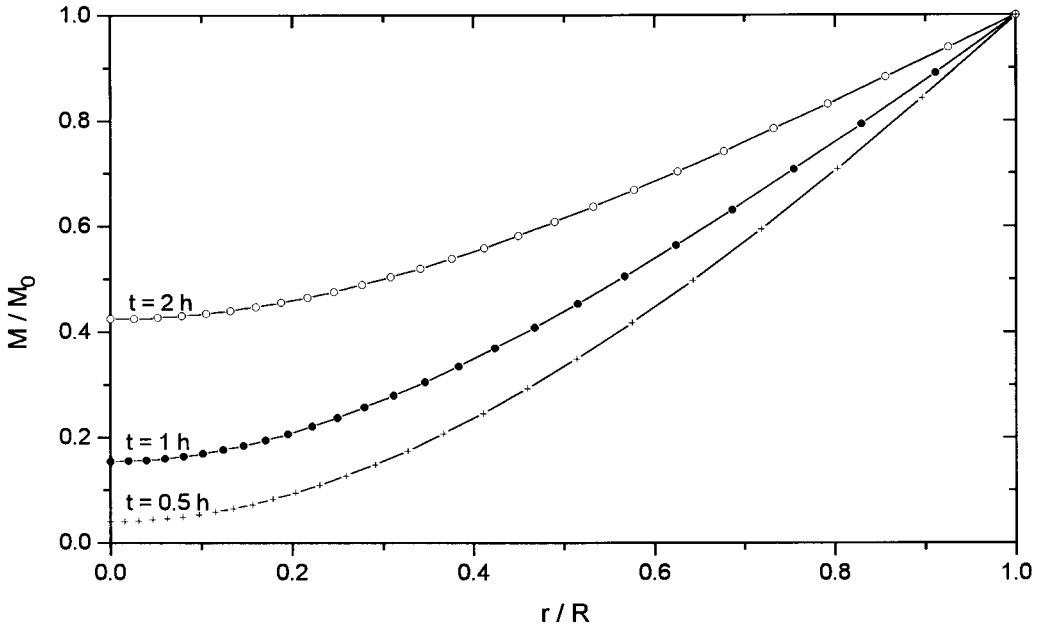

Figure 4 Effect of reaction time on the radial profiles of butadiene in polymeric particle. $k_p^0 = 1.6 \times 10^9$ m^3/s mol sites, $E_A = 2.4 \times 10^4$ J/mol, $C_0^* = 1.8 \times 10^{-1}$ mol sites/kg cat, $R_0 = 25$ μm, $T'_{\text{gas}} = 323$ K, $p_{\text{BD}} = 2.35 \times 10^5$ Pa, $D_e = 2.6 \times 10^{-10}$ m^2/s.

with radius of 37 μm was measured on-line by a video microscope. The reactor was a nonisothermal system.

The multilayer model with deactivation of the active sites can be reasonably used to simulate the rate of polymeric particle growth for the gas phase polymerization of butadiene comparatively well (Fig. 8). Among the simulation results, simulation (b) is comparatively good in accord with the experimental result. However, Figure 8 shows

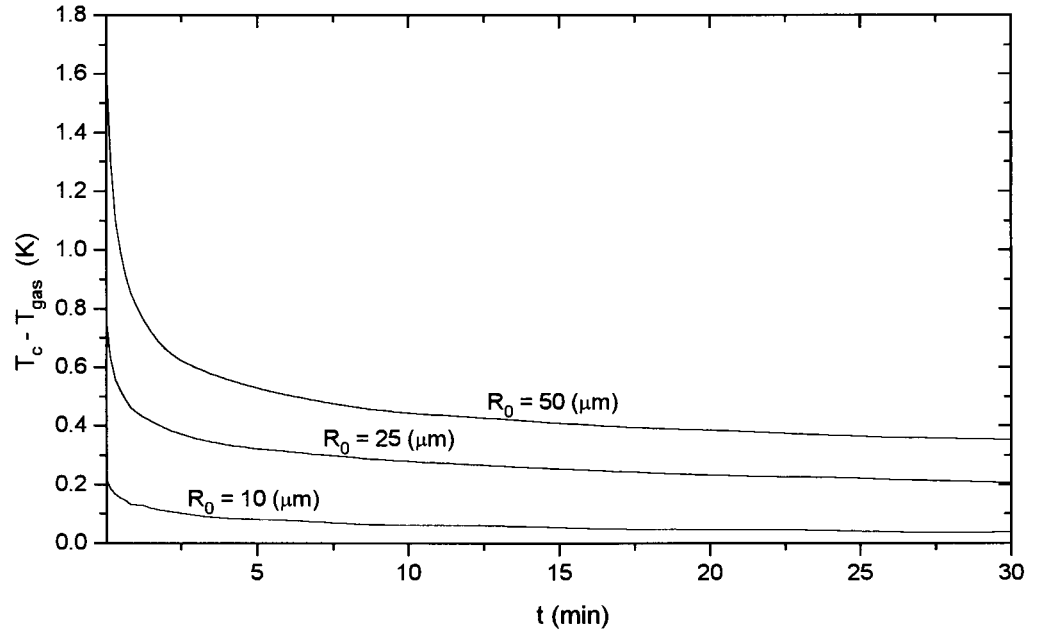

Figure 5 Temperature rise of polymeric particle vs. time. $k_p^0 = 1.6 \times 10^9$ m^3/s mol sites, $E_A = 2.4 \times 10^4$ J/mol, $C_0^* = 1.8 \times 10^{-1}$ mol sites/kg cat, $D_e = 2.6 \times 10^{-10}$ m^2/s, $T_{\text{gas}} = 323$ K, $p_{\text{BD}} = 2.35 \times 10^5$ Pa, $u = 0$ m/s.

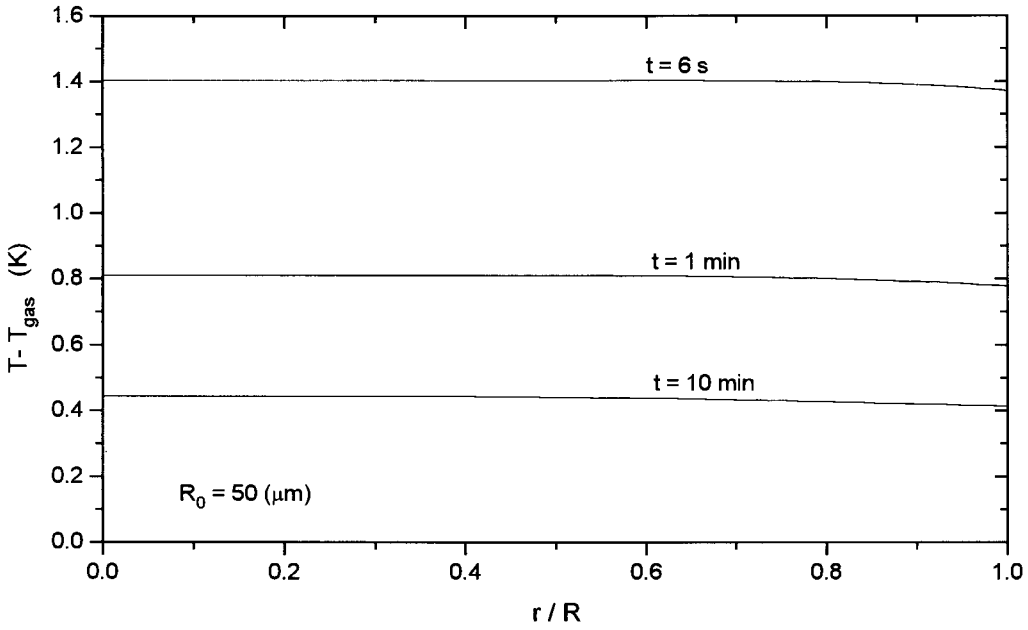

Figure 6 Profile of temperature in polymeric particle. $k_p^0 = 1.6 \times 10^9$ m^3/s mol sites, $E_A = 2.4 \times 10^4$ J/mol, $C_0^* = 1.8 \times 10^{-1}$ mol sites/kg cat, $D_e = 2.6 \times 10^{-10}$ m^2/s, $R_0 = 50$ μm, $T_{\text{gas}} = 323$ K, $p_{\text{BD}} = 2.35 \times 10^5$ Pa, $u = 0$ m/s.

that there is still a difference between the simulation results and the experimental result. From simulation (a), in which a low value of D_e is used, one can see that it is not reasonable to use molecular diffusivity to simulate the rate of particle growth. For the experimental curve, from the beginning of reaction to about 0.5 h, the rate of particle growth is speeded up significantly. It is more

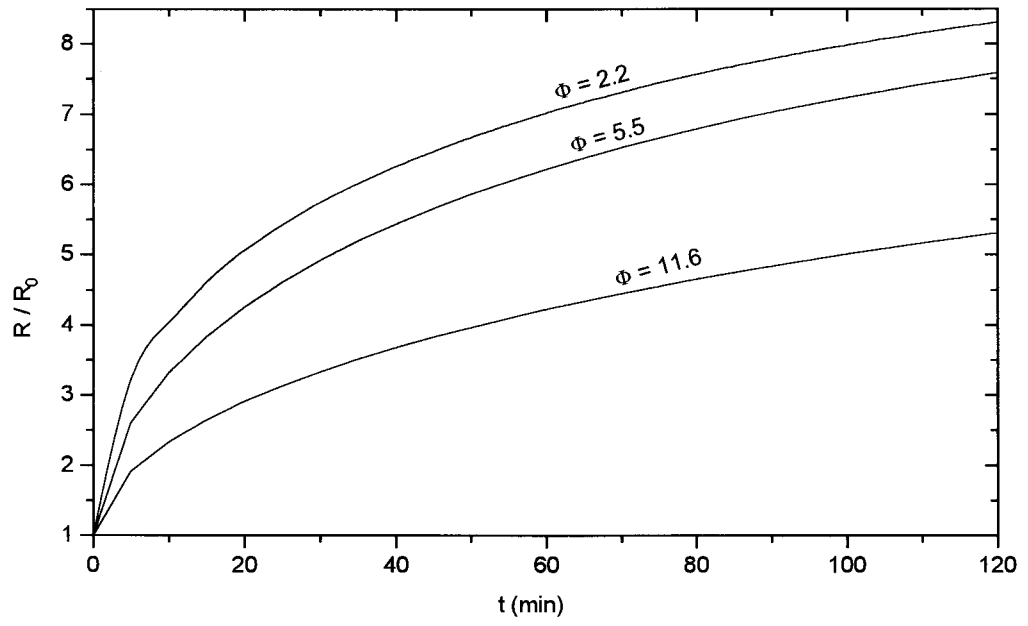

Figure 7 Effect of Thiele modulus on the rate of polymeric particle growth. $k_p^0 = 1.6 \times 10^9$ m^3/s mol sites, $E_A = 2.4 \times 10^4$ J/mol, $C_0^* = 1.8 \times 10^{-1}$ mol sites/kg cat, $T_{\text{gas}} = 323$ K, $p_{\text{BD}} = 2.35 \times 10^5$ Pa; the curve with $\Phi = 2.2$: $R_0 = 10$ μm, $D_e = 5 \times 10^{-10}$ m^2/s; the curve with $\Phi = 5.5$: $R_0 = 25$ μm, $D_e = 5.0 \times 10^{-10}$ m^2/s; the curve with $\Phi = 11.6$: $R_0 = 10$ μm, $D_e = 2.0 \times 10^{-11}$ m^2/s.

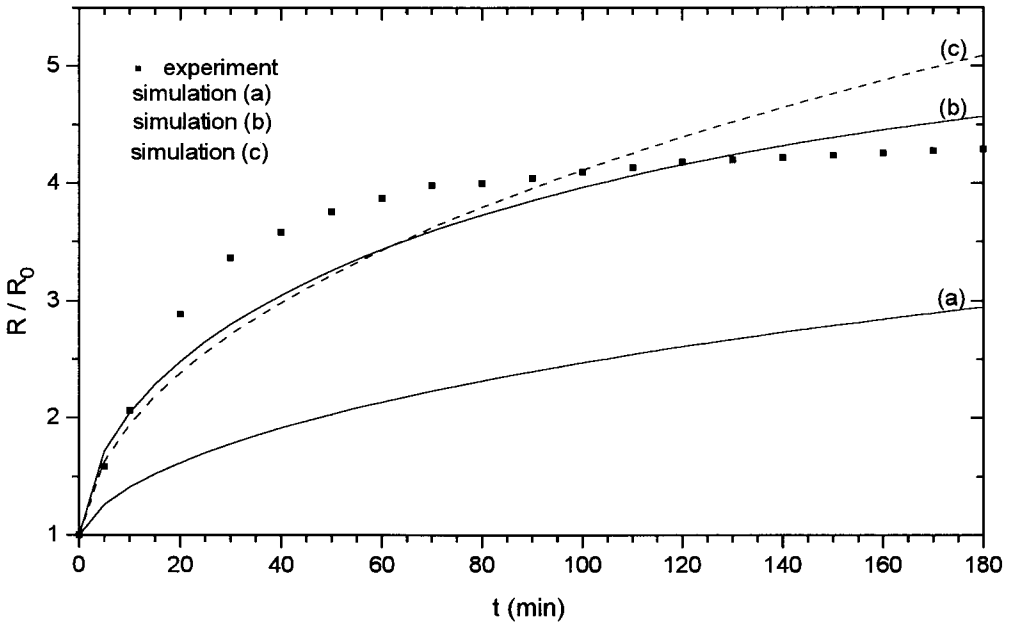

Figure 8 Comparison of the simulation results with experimental results of polymeric particle growth. $k_p^0 = 1.6 \times 10^9$ m^3/s mol sites, $E_A = 2.4 \times 10^4$ J/mol, $C_0^* = 1.8 \times 10^{-1}$ mol sites/kg cat, $R_0 = 37$ μm, $p_{BD} = 2.7 \times 10^5$ Pa; simulation (a): $T_{gas} = 297$ K, $D_e = 1.0 \times 10^{-11}$ m^2/s; simulation (b): $T_{gas} = 323$ K, $D_e = 1.0 \times 10^{-10}$ m^2/s; simulation (c): $T_{gas} = 297$ K, $D_e = 1.0 \times 10^{-10}$ m^2/s; experiment: initial temperature of gas phase = 297 K, $p_{BD} = 2.7 \times 10^5$ Pa, $R_0 = 37$ μm, $C_0^* = 1.8 \times 10^{-1}$ mol sites/kg cat.

likely that a significant temperature rise in the gas phase of the reactor is the main cause of the speeding up of the rate of particle growth at the beginning of polymerization. The experimental curve of the rate of particle growth flattens at the later period of reaction. One cause of this phenomena may be the deactivation of active sites, and the other more likely may be the significant temperature decline of the gas phase in the reactor at the later period of reaction.

CONCLUSIONS

The polymeric multilayer model with heat transfer resistance at the external boundary layer can describe reasonably well the process of heat transfer at the external film and intraparticle heat transfer resistance of the gas phase polymerization of butadiene. The simulation results predict that, for the gas phase polymerization of butadiene under the conditions discussed, no serious temperature rise in the polymeric particle is to be expected and the temperature profile in the polymeric particle is almost uniform; that is, it is unlikely to expect overheating of the polymeric particle of the gas phase polymerization of butadiene, even with a comparatively large catalyst particle.

The intraparticle mass transfer limitation is significant, especially for a comparatively large catalyst particle, which can likely lead to a broad molecular weight distribution.

The model can simulate reasonably well the rate profile of polymeric particle growth. The simulation results do correspond with the experimental result in spite of some differences at different levels of polymerization.

The first author would like to thank the Foundation of Pao Yu-Kong and Pao Zhao-Long Scholarship for Chinese Students Studying Abroad for financial support during his stay in Germany.

NOMENCLATURE

A_j	radial discretization weight
B_j	radial discretization weight
B_0	coefficient
C_j	radial discretization weight
C_0^*	initial concentration of active sites (mol sites/kg cat)

C^* concentration of active sites (mol sites/kg cat)
$C_j^{*(i)}$ concentration of active sites based on volume of layer in layer j at time i (mol sites/m^3)
C_p heat capacity of polymeric particle (J/kg K)
C_{PBR} heat capacity of polymer (J/kg K)
$C_{p\,cat}$ heat capacity of catalyst (J/kg K)
$C_{p\,gas}$ heat capacity of gas-phase bulk (J/kg K)
d_p diameter of polymer particle (m)
D_e effective diffusion coefficient of monomer in polymeric particle (m^2/s)
D_m molecular diffusion coefficient of butadiene in polybutadiene (m^2/s)
E_A activation energy for propagation (J/mol)
E_D activation energy of deactivation (J/mol)
ΔH_p heat of polymerization (J/mol)
h external film heat transfer coefficient (W/m^2 K)
k_{BR} thermal conductivity of polymer (W/m K)
k_e thermal conductivity of polymeric particle (W/m K)
k_{gas} thermal conductivity of gas-phase bulk (W/m K)
k_p propagation rate constant (m^3/s mol sites)
k_p^0 frequency factor of propagation (m^3/s mol sites)
k_d deactivation rate constant (1/s)
k_d^0 frequency factor of deactivation (1/s)
M monomer concentration (mol/m^3)
M_0 monomer concentration in bulk of gas phase (mol/m^3)
M_m molecular weight of butadiene
N total number of grid points or layers plus 1
Nu Nusselt number
p_{BD} partial pressure of butadiene in gas phase (Pa)
Pr Prandtl number
Q_p total heat of polymerization (W/m^3)
r radial position in growing polymeric particle (m)
R_0 radius of catalyst (m)
R radius of polymeric particle (m)
Re Reynolds number
R_p polymerization rate (mol/s m^3)
t reaction time (s)
Δt time increment for numerical solution (K)
T temperature in polymeric particle (K)
T_c temperature at the center of polymeric particle (K)
T_{gas} temperature in bulk of gas phase (K)
u particle–fluid relative velocity (m/s)
$V_j^{(i)}$ volume of layer j at time i (m^3)

Greek Symbols

μ_{gas} viscosity of gas-phase bulk (Pa s)
ρ_p density of polymeric particle (kg/m^3)
ρ_{gas} density of gas-phase bulk (kg/m^3)
ρ_{cat} density of catalyst (kg/m^3)
ρ_{BR} density of polymer (kg/m^3)
Φ Thiele modulus = $R_0\sqrt{k_p C_0^* \rho_{cat}/D_e}$

REFERENCES

1. B. Garmatter, diploma thesis, Technical University of Berlin, 1995.
2. C. Eberstein, B. Garmatter, K.-H. Reichert, and G. Sylvester, *Gasphasenpolymerisation von Butadien, Chemie Ingenieur Technik,* **68,** 820 (1996).
3. D. Singh and R. P. Merrill, *Macromolecules,* **4,** 599 (1971).
4. V. W. Buls and T. L. Higgins, *J. Polym. Sci.: Part A1,* **8,** 1037 (1970).
5. E. J. Nagel, V. A. Kirilov, and W. H. Ray, *Ind. Eng. Chem. Product Res. Dev.,* **19,** 372 (1980).
6. S. Floyd, K. Y. Choi, T. W. Taylor, and W. H. Ray, *J. Appl. Polym. Sci.,* **31,** 2231 (1986).
7. S. Floyd, K. Y. Choi, T. W. Taylor, and W. H. Ray, *J. Appl. Polym. Sci.,* **32,** 2935 (1986).
8. R. A. Hutchinson, C. M. Chen, and W. H. Ray, *J. Appl. Polym. Sci.,* **44,** 1389 (1992).
9. J. B. P. Soares and A. E. Hamielec, *Polym. Reaction Eng.,* **3,** 261 (1995).
10. J. Crank, *The Mathematics of Diffusion,* 2nd ed., Oxford University Press, New York, 1990, p. 316.
11. G. F. Froment and B. Bischoff, *Chemical Reactor Analysis and Design,* Wiley, New York, 1979.
12. W. E. Ranz and W. R. Marshall, Jr., *Chem. Eng. Prog.,* **48,** 141 (1952).
13. J. Brandrup and E. H. Immergut, *Polymer Handbook,* 3rd ed., Wiley, New York, 1989.
14. D. W. Van Krevelen, *Properties of Polymers,* 2nd ed., Elsevier Science Publishers B. V., The Netherlands, 1986.
15. H. T. Ba, diploma thesis, Technical University of Berlin, 1995.
16. R. W. Gallant, *Physical Properties of Hydrocarbons,* Vol. 1, Gulf, Houston, 1970.